Eur Biophys J (1996) 24: 243–250

European Biophysics Journal

EXAFS investigation of the active site of iron superoxide dismutase of *Escherichia coli* and *Propionibacterium shermanii*

C. Scherk [1], M. Schmidt [1], H.-F. Nolting [3], B. Meier [2], F. Parak [1]

[1] Fakultät für Physik E17, Technische Universität München, D-85747 Garching, Germany
[2] Chemisches Institut, Tierärztliche Hochschule Hannover, Bischofsholer Damm 15, D-30173 Hannover, Germany
[3] EMBL c/o DESY, Notkestrasse 85, D-22603 Hamburg, Germany

Received: 13 November 1995 / Accepted: 29 January 1996

Abstract. The local structure of the iron site in ferric superoxide dismutase from *P. shermanii* was analyzed by X-ray absorption spectroscopy. The metal-ligand cluster of the enzyme is found to be similar to the crystallographically investigated ferric superoxide dismutase from *E. coli*. At pH 6.4 the enzyme is five-fold coordinated with three histidines, an aspartate and a water molecule. The average bond lengths between the metal and the histidines are about 2.10 Å, between metal and aspartate they are about 1.86 Å and between metal and water 1.96 Å. With an increase in pH a change in the coordination number from five to six is observed both in pre-edge peak and EXAFS spectra analysis. However, the bond lengths of the ligands do not change dramatically, they are conserved for the aspartate and increase slightly to 2.13 Å for the average metal – histidine distance at pH 9.3. The observation of the increase in coordination number is correlated with a decrease in enzymatic activity which occurs in the high pH range. The zinc EXAFS spectra of *P. shermanii* superoxide dismutase have shown that zinc can be incorporated in the active center instead of the iron.

Key words: Iron superoxide dismutase – SOD – X-ray absorption – XAS – Extended X-ray absorption fine structure – EXAFS – *P. shermanii* – *E. coli* – Metalloproteins

Introduction

Superoxide dismutases (SOD; EC 1.15.1.1) are metalloproteins that catalyze the dismutation of the biologically toxic superoxide ions into oxygen and hydrogen peroxide:

$$Me_{Ox} + O_2^- \rightarrow Me_{Red} + O_2,$$
$$Me_{Red} + O_2^- + 2\,H^+ \rightarrow Me_{Ox} + H_2O_2.$$

Three types of the enzyme are known depending on the metal, Me, contained in the active center: the copper/zinc, the iron and the manganese SODs. The Cu/Zn-SODs are found primarily as dimers in the cytosol of eukaryotic cells and contain one copper and one zinc ion per 17 kDalton monomer (Tierney et al. 1995). The iron and manganese containing SODs are widely distributed in bacteria and in the mitochondria of eukaryotes. These enzymes form either dimers or tetramers with molecular masses between 19 and 23 kDalton per monomer. The reaction rate for the dismutation of the superoxide ion is about 10^9 $M^{-1}s^{-1}$ (Meier et al. 1994). The X-ray structures of the Mn-SOD of *Thermus thermophilus* (Stallings et al. 1985; Ludwig et al. 1991) and of the Fe-SOD of *Pseudomonas ovalis* (Stoddard et al. 1990; Ringe et al. 1983) and of *Escherichia coli* (Tierney et al. 1995; Stallings et al. 1983) were determined at high resolution and show strong structural similarities (Stallings et al. 1984). The Fe(III) is five-coordinate in trigonal bipyramidal geometry. In all cases the metal ion is coordinated by three histidine nitrogens and an aspartate oxygen. Furthermore, recent publications indicate the presence of a water molecule as an additional fifth ligand (Ludwig et al. 1991; Tierney et al. 1995).

In this paper we describe the investigation of the environment of the active center of the Fe-SOD of the anaerobic living, cambialistic *Propionibacterium shermanii subspec. freudenreichii*. This SOD consists of two monomers of 23 kDalton. Each monomer has one active center which contains an iron atom in the ferric state (Tainer et al. 1982). The activity of the SOD depends strongly on pH and decreases with increasing pH value (Meier et al. 1995). The iron of this SOD can be replaced by Mn without destroying the catalytic activity (Meier et al. 1982). Additionally, the SOD builds inactive forms where the iron is replaced by copper, cobalt or zinc atoms. The cambialistic behavior is demonstrated by Fig. 1, which shows a fluorescence radiation spectrum of the *P. shermanii* SOD sample. The characteristic lines of the various cations at the active center are clearly visible.

Extended X-ray absorption fine structure (EXAFS) provides a sensitive probe of the local structural environment of the metal in metalloproteins. The technique is non-destructive, atom specific and does not depend on the state

Correspondence to: F. Parak

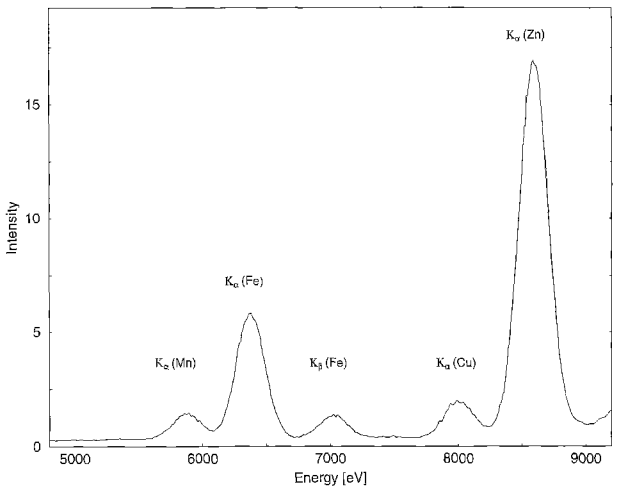

Fig. 1. X-ray fluorescence emission spectrum of a *P. shermanii* SOD sample after excitation with monochromatic synchrotron radiation at 10000 eV

of aggregation of the sample. Since it is no problem to vary the pH-values or the temperature of the probes, EXAFS is a complementary technique to crystallographic studies and allows the observation of structural changes which would destroy single crystals. However, the EXAFS technique gives rise to particular problems. The resolution of the spectra of biological samples is limited since the oscillations decrease rapidly with energy. This is because of the low backscattering power of the ligand atoms such as oxygen, nitrogen and carbon and, in part, because of the low concentration of the absorbing atoms. Additionally, the geometry of the active site is often not precisely defined owing to conformational substates (Parak and Frauenfelder 1993). Without additional information it is not possible to fit the coordinates of the neighbor atoms of the metal center unambiguously to the EXAFS spectra. In order to come to a unique interpretation, an EXAFS spectrum of the SOD of *E. coli* has been measured as well. For this Fe-SOD the X-ray structure is available (Lah et al. 1995). The X-ray coordinates are taken as starting parameters for the EXAFS interpretation of the *E. coli* Fe-SOD. The refined EXAFS results of the *E. coli* Fe-SOD is in turn used to get starting coordinates for the interpretation of the EXAFS spectra of *P. shermanii* SOD. It should be mentioned that the X-ray structure of the SOD of *P. shermanii* is in progress in our group.

Materials and methods

E. coli Fe-SOD was purchased from Sigma chemical company. It was purified by FPLC and concentrated to 200 mg/ml at pH 8.0 by ultrafiltration with Centricons microconcentrators. The SOD of *P. shermanii* was extracted from Propionibacteria grown on a complex medium. After purification, three different pH-values were established by dialysation against MES/TRIS buffer (25 mM) at pH 6.4 and against TRIS/HCl buffer (25 mM) at pH 7.8 and at pH 9.3. Finally the SOD solutions were concentrated up to 120 mg/ml.

X-ray absorption measurements were carried out at EMBL at the beamline D 2, EXAFS I in Hamburg, Germany, using a Si(111) double monochromator with a double focusing mirror. The absorption data were recorded as fluorescence excitation spectra with a 13 NaI scintillation counter array. The samples were frozen in liquid nitrogen and kept at a temperature of 20 K during the EXAFS measurements. Spectra were recorded in the energy region between 6900 and 7800 eV. After the measurements the energy axis of the EXAFS spectra was calibrated by reflections of a Silicon crystal (Pettifer and Hermes 1985). Artifacts in individual detector channels resulted in the exclusion of this channel. The acceptable channels of the detector were subsequently summed. The individual scans of the energy region were repeated until the total number of fluorescence counts above the absorption edge accumulated to about 700000 for the *E. coli* SOD.

Data evaluation and results

In a first step the pre-edge region of the absorption spectra was analyzed. Below the edge jump a first order polynomial was fitted to the experimental data between 7030 and 7080 eV which accounted for the background noise. It was subsequently subtracted from the total spectrum. Above the edge jump a fourth order polynomial was fitted to the data. It was used to normalize the intensity in this region of the spectrum to one. The 1s $\rightarrow$ 3d pre-edge transition intensity was separated by fitting a first order polynomial plus an arctangens to the regions below (7098.0 to 7107.0 eV) and above (7115.5 to 7118.5 eV) this transition region. The pre-edge area was subsequently calculated by integrating the difference between the normalized experimental data and the fitted curve in the energy window from 7110.0 to 7115.0 eV. The coordination number of the investigated complex can be estimated by comparison of the transition intensity to empirical values available for several ferric complexes (Roe et al. 1984). In general, the area of the transition intensity increases from six-coordinate pseudooctahedral ($<10\times10^{-2}$ eV) through five-coordinate (12 to 19×10^{-2} eV) to four-coordinate pseudotetrahedral ($>23\times10^{-2}$ eV).

Above the edge (7140 to 7570 eV) the EXAFS function $\chi(E)$ which reflects only the oscillatory part of the absorption data $\mu(E)$ was extracted. A background substraction was accomplished by fitting once again a first order polynomial to the region below the edge (7030 to 7080 eV). Above the edge (7140 to 7820 eV) a spline function through four equidistant data points accounted for the non-oscillatory part of the absorption which represented the vacuum absorption of an iron atom $\mu_0(E)$. With this spline, $\chi(E)$ could be calculated $\chi(E)=(\mu(E)-\mu_0(E))/\mu_0(E)$. The data were converted from energy to k space using $k=\sqrt{2m_e(E-E_0)/\hbar^2}$. E_0 represents the ionization energy of a K electron of the iron atom and was set to 7120 eV, m_e is the electron mass.

EXAFS data analysis was performed using the computer program EXCURV92 (Binsted et al. 1991). This program calculates a theoretical EXAFS spectrum and uses a

Marquart routine to fit iteratively the theoretical curve to the experimental data. Scattering amplitudes and phase shifts are computed ab initio with the use of Hedin-Lundquist potentials (Lee and Beni 1977). The theoretical function is calculated by a rapid curved wave theory which includes up to triple multiple scattering contributions. Usually only radial distances are taken into account in EXAFS data evaluation. But if the calculations of the spectra apply a multiple scattering theory a three-dimensional structure with all angles and interatomic distances should be introduced. It has been shown explicitly that the multiple scattering inside the imidazole rings can account for rather strong contributions to the EXAFS function (Strange et al. 1987). Therefore, a three dimensional structure consisting of all the atoms surrounding the absorbing atom is required as input into the program in order to extract the maximum amount of information contained in the EXAFS spectrum. Other parameters that are essential for the fitting procedure are the amplitude reduction factor, *AFAC*, which reflects an EXAFS intensity loss due to shake up/off processes in the absorbing atom and the mean square displacements, σ^2, which are used to calculate Debye-Waller factors. The *AFAC* of iron was computed for $k \geq 7$ Å^{-1} and set equal to 0.69 (Teo 1986).

Two refinement techniques have been used (Binsted et al. 1992). In the "constrained refinement", groups of atoms are defined as units (here: the three imidazole rings, the atoms of the carboxyl group of the aspartate and the water molecule). These units are allowed to move only as a whole without changing the intragroup distances. Therefore, fitting parameters are only the distances between the nearest atom of each group and the iron atom and two angles defining the orientation of these units respective to the iron. This approach is validated by the stable, well defined internal geometry of the groups. In the "restrained refinement" all distance parameters are varied but restraints are set inside the units that were defined above. These restraints are crystallographically determined ideal distances of, e. g., the atoms forming the imidazole rings. The deviations of these values from their standards are introduced into the minimization routine of the fitting procedure.

E. coli ferric SOD

Figure 2 shows the normalized absorption edges for *E. coli* at pH 8.0 and *P. shermanii* at pH 7.8. Although these spectra show an overall similarity the noticeable difference cannot be disregarded. The oscillations of the EXAFS spectrum of *P. shermanii* are far more pronounced while the pre-edge peak is drastically reduced. The 1s→3d transition which is forbidden according to spectral selection rules can be interpreted in terms of quadrupole and symmetry breaking effects (Shulman et al. 1976) and is correlated with the geometry of the absorber coordination sphere. Its analysis gives an area of 14.0×10^{-2} eV for the *E. coli* Fe-SOD (see Table 1) which accounts for a five-fold coordination of the iron (Roe et al. 1984). Another group which performed similar EXAFS measurements of the *E. coli* Fe-SOD (Tierney et al. 1995) obtained the same

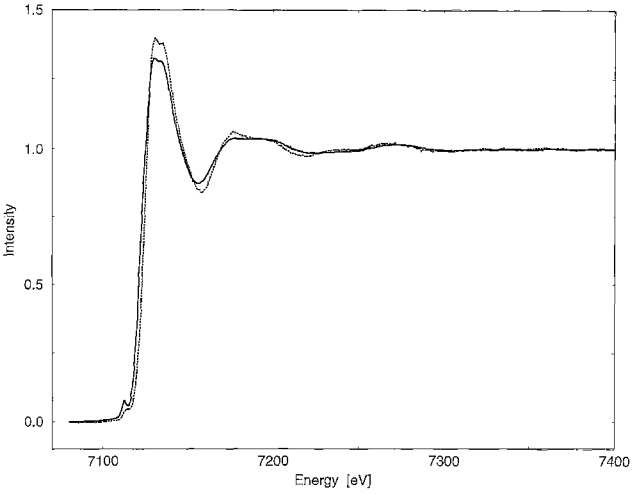

Fig. 2. Normalized X-ray absorption spectra of the *E. coli* Fe-SOD at pH 8.0 (*solid line*) and the *P. shermanii* Fe-SOD at pH 7.8 (*dotted line*)

Table 1. Peak areas of the 1s→3d pre-edge transition for the *E. coli* and *P. shermanii* ferric SOD. The peak areas reflect the difference of the experimental data and a fitted first order polynomial and an arctangens that are integrated between 7110.0 and 7115.0 eV

Pre-edge peak analysis		Peak area [10^{-2} eV]
E. coli	pH 8.0	14.0
P. shermanii	pH 6.4	11.5
	pH 7.8	7.1
	pH 9.3	6.3

result in this pH range, which also coincides with the crystallographic structure (Lah et al. 1995). The crystallographic data from the X-ray structure analysis at pH 7.0 (Protein data bank file: pdb1isb.ent, resolution 1.85 Å) are taken as a reference level for the EXAFS refinement procedure. The coordinates of the two crystallographically not completely identical active sites of the dimer structure are averaged and put into the EXAFS analyzing program (see Table 2, Fig. 3). Since multiple scattering contributions should be included in the EXAFS data evaluation, all the atoms within a sphere of radius 4 Å are taken into account. Thus the atoms included are three complete imidazole rings (2 nitrogen and three carbon atoms each), the carboxyl group of the aspartate (2 oxygen and 1 carbon) and a water molecule modeled by a single oxygen. It was verified by simulations that the hydrogen atoms give no significant scattering contributions and thus can be excluded in the presentation of the water molecule.

Figure 4 compares experimental and theoretical k^3 weighted EXAFS curves. The theoretical curve is calculated from the original X-ray structure of *E. coli* Fe-SOD with fixed mean square displacements, σ_i^2, ($\sigma^2{}_{1-19} = 0.0025$ Å^2, representing the mean square displacements of atom 1 through 19 defined in Table 2). It is evident that the two curves coincide only roughly. In particular, the Fourier transform of the spectrum (Fig. 5) shows significant differences. To improve the agreement a refinement was performed where the mean square displacements, σ_i^2,

Table 2. Coordinates of the X-ray structure of *E. coli* ferric SOD (Lah et al. 1995). Bold letters refer to the atoms of the first coordination shell. Row 1 shows type and number of the atoms, row 2/3 the ligand type as defined in the PDB. Rows 4 and 5 show the exact radial positions of the atoms in each active site of the dimer. Rows 6–8 give the averaged coordinates over these almost identical sites. A spherical coordinate system centered at the iron atom ($\vartheta=0$ determines the positive z-achses, $\varphi=0$, $\vartheta=\pi/2$ the positive x-achses of the Cartesian coordinate system in Fig. 3) is used

Atom	PDB code		Radius R [Å] X-ray site A	Radius R [Å] X-ray site B	Radius R [Å] sites averaged	ϑ [°] averaged	φ [°] averaged
Fe_0	FE		$R_0(Fe)=0.00$	0.00	0.00	0.00	0.00
O_1	**ASP**	**OD2**	**$R(O_1)=1.89$**	**1.93**	**1.91**	26.85	191.09
C_2	ASP	CG	$R_2=2.99$	3.01	3.00	12.93	181.90
O_3	ASP	OD1	$R_3=3.44$	3.43	3.44	10.91	61.52
N_4	**HIS I**	**NE2**	**$R(N_4)=2.15$**	**2.17**	**2.16**	111.68	180.00
C_5	HIS I	CE1	$R_5=3.11$	3.12	3.11	91.46	176.36
C_6	HIS I	CD2	$R_6=3.09$	3.11	3.10	131.84	175.03
N_7	HIS I	ND1	$R_7=4.21$	4.22	4.22	101.74	172.71
C_8	HIS I	CG	$R_8=4.24$	4.24	4.24	119.73	171.48
N_9	**HIS II**	**NE2**	**$R(N_9)=2.06$**	**2.03**	**2.05**	112.98	285.49
C_{10}	HIS II	CE1	$R_{10}=3.02$	3.05	3.03	106.92	305.67
C_{11}	HIS II	CD2	$R_{11}=3.01$	2.92	2.97	109.93	261.60
N_{12}	HIS II	ND1	$R_{12}=4.13$	4.12	4.12	106.00	293.49
C_{13}	HIS II	CG	$R_{13}=4.15$	4.09	4.12	107.23	274.23
N_{14}	**HIS III**	**NE2**	**$R(N_{14})=2.08$**	**2.06**	**2.07**	112.69	79.80
C_{15}	HIS III	CE1	$R_{15}=3.07$	3.03	3.05	111.46	58.15
C_{16}	HIS III	CD2	$R_{16}=3.00$	3.02	3.00	107.61	102.15
N_{17}	HIS III	ND1	$R_{17}=4.17$	4.15	4.16	110.14	70.41
C_{18}	HIS III	CG	$R_{18}=4.18$	4.18	4.18	108.46	89.82
O_{19}	**H_2O**	**HOH**	**$R(O_{19})=1.92$**	**1.99**	**1.96**	64.08	0.41

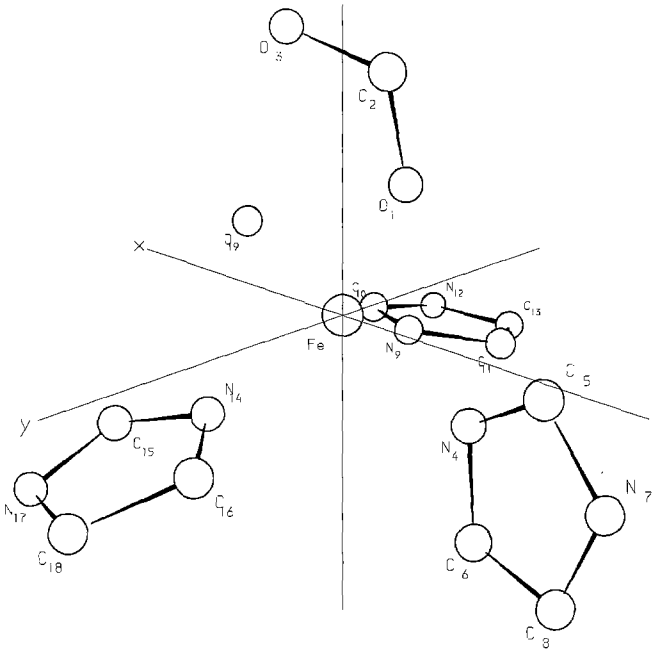

Fig. 3. Geometry of the atoms which form the active center of the *E. coli* Fe-SOD (Lah et al. 1995). These atoms are used for the simulation of the EXAFS data. The carboxyl group of an aspartate (atoms 1 to 3), the imidazole rings of three histidines (atoms 4 to 18) and a water molecule (atom no. 19) are shown

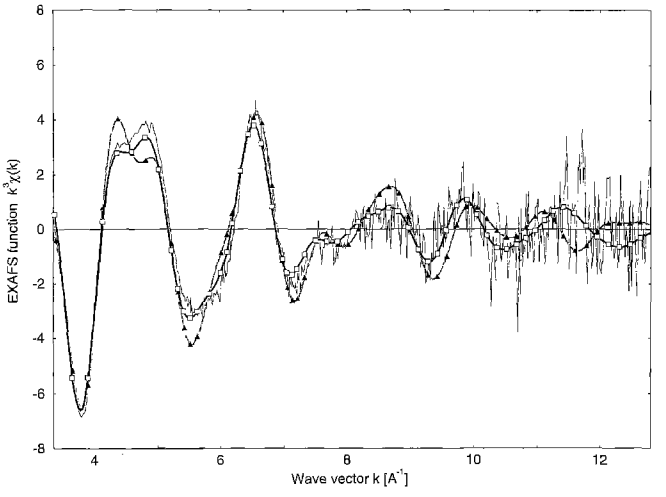

Fig. 4. EXAFS spectrum of *E. coli* Fe-SOD at pH 8.0 (*thin solid line*) compared to calculated functions; triangles: coordinates from the unrefined X-ray structure of *E. coli* with constant mean square displacements (see Table 2); squares: "restrained refinement" analysis. Distances of the atoms in the first coordination shell as defined in Table 2: $R(O_1)=1.86$ Å, $R(N_4)=2.15$ Å, $R(N_9)=2.05$ Å, $R(N_{14})=2.07$ Å, $R(O_{19})=1.97$ Å

were allowed to vary. This simulation yielded slight improvements but produced unrealistic σ_i^2-values of some atoms. This shows that the differences in the spectra do not stem from miscalculated Debye-Waller factors but that the X-ray structure does not reflect the geometry correctly enough. To avoid the strong influence of Debye-Waller factors in the further simulations the mean square displacements were fixed again. They were used to minimize the deviation of the refined distances of the first coordination shell atoms with regard to the X-ray structural data. The chosen σ_i^2-values are of the same order of magnitude as determined for myoglobin by RSMR measurements and optical absorption spectroscopy (Achterhold 1995; Di Pace et al. 1992). The mean square displacements of the atoms of the imidazole rings and the carboxyl group

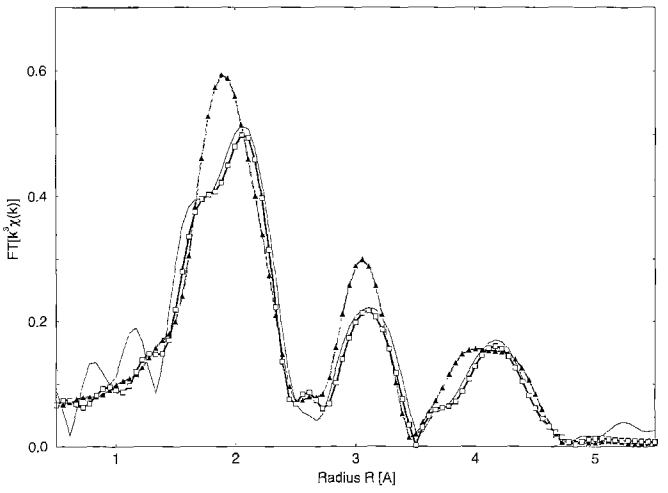

Fig. 5. Fourier transform of the *E. coli* Fe-SOD EXAFS spectra at pH 8.0 (*thin solid line*); *triangles:* theoretical curve calculated from the unrefined X-ray structure of *E. coli* Fe-SOD (see Table 2); *squares:* after a "restrained refinement" analysis. Distances of the atoms in the first coordination shell as defined in Table 2: $R(O_1)=1.86$ Å, $R(N_4)=2.15$ Å, $R(N_9)=2.05$ Å, $R(N_{14})=2.07$ Å, $R(O_{19})=1.97$ Å

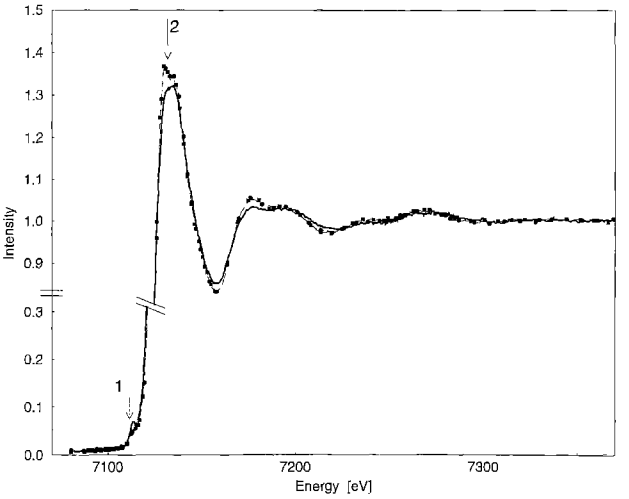

Fig. 6. X-ray absorption spectra of the *P. shermanii* Fe-SOD at different pH-values; *thick-sold line:* pH 6.4, *circles:* pH 7.8, *squares:* pH 9.3

reflecting the first coordination shell were set to σ_1^2, σ_4^2, σ_9^2, $\sigma_{14}^2=0.0015$ Å^2, those of the other atoms to 0.0025 Å^2. The strategy of not varying individual Debye-Waller factors for the different atoms in the first refinement step is commonly used in the X-ray structure determination of proteins.

In a further step, the structure was refined using the "constrained refinement" method. The first maximum of the Fourier transformed spectra can be reproduced quite reasonably but the total fit remain unsatisfactory. Obviously the general arrangement of the defined units is displayed correctly by the X-ray structure except for the aspartate which moves closer to the iron atom ($R_1=1.85$ Å). This result is confirmed by the angular information obtained from the multiple scattering contributions. The deviations of all angles after the refinement compared to the original X-ray structure remain below two degrees. This is also true for the analysis of all other EXAFS spectra reported here.

In a third attempt the "restrained refinement" method was used. The standard values of the atomic distances within the imidazole rings of the histidines and the carboxyl group of the aspartate were taken from the library of the "O program" (Jones 1994) used in protein crystallography. During the fitting procedure all the distances with respect to the iron atom were varied except the distances of the nearest atoms of histidines II and III. This way the correlation between these identical groups was reduced. Astonishingly, the refined structure (see Fig. 4 and Fig. 5) yields atomic distances within the histidines and the aspartate which are even closer to the introduced standard values than those of the X-ray structure analysis (Lah et al. 1995). Nevertheless, the maximum discrepancy between the refined and the standard values is always smaller than 0.02 Å. The imidazole rings remain practically at the position obtained by the X-ray structure analysis. However, the aspartate is shifted closer to the iron. This shift accounts for the asymmetry for the first coordination shell expressed in the Fourier transform (see Fig. 5).

P. shermanii ferric SOD

The refined structure of the *E. coli* Fe-SOD was used as the starting for the analysis of the structure of the active center of the SOD of *P. shermanii.* The amplitude reduction factor, *AFAC,* and the mean square displacements, σ^2, were fixed at the values that had proved to be optimal for the *E. coli* Fe-SOD in the first step.

The absorption spectra of *P. shermanii* SOD at pH 7.8 and pH 9.3 are practically identical (compare Fig. 6). Differences can be seen between pH 6.4 and pH 7.8. At pH 7.8 the amplitude of the EXAFS oscillations is increased while the pre-edge transition has lost intensity. The 1s→3d pre-edge transition (see Fig. 7 and Table 1) is less pronounced for all pH-values than for the *E. coli* SOD. At pH 6.4 this indicates a coordination between five- and six-fold. The transition area decreases for the higher pH-values and gives here a clear hint for six-fold coordination.

For an interpretation of the pH 6.4 EXAFS data we started with the coordinates obtained from the *E. coli* EXAFS data refinement. Good agreement is only obtained for $k\leq 7.5$ Å^{-1}. Then the "constrained refinement" method was applied. In this case the only fitting parameters were the radial distances of each group and, additionally, three angles defining the orientation of one imidazole ring each. The angles were chosen in a way that each imidazole ring was allowed to turn in a plane determined roughly by the imidazole ring plane itself and the iron atom. The nitrogen atom which is closest to the iron atom was used as pivot. The additional degree of freedom perpendicular to this plane was omitted. A very good fit for pH 6.4 can be achieved with this model (compare Fig. 8). A "restrained refinement" does not improve the quality significantly. From the EXAFS point of view the SOD of *E. coli* at pH 8.0 and the SOD of *P. shermanii* are very similar at the

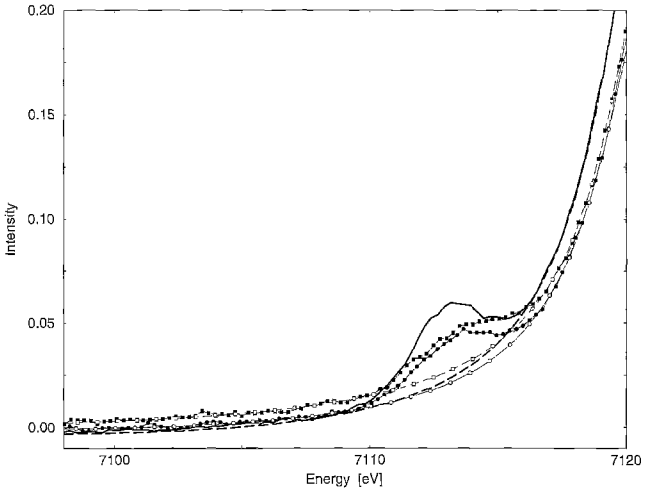

Fig. 7. Analysis of the peak areas of the 1s→3d pre-edge transition of *P. shermanii* Fe-SOD; *thick solid line:* the experimental spectra at pH 6.4; *circles:* pH 7.8, *squares:* pH 9.3. The fitted background functions are displaced accordingly (*dashed lines*). The difference between experimental and background spectra are used to determine the coordination number of the absorbing atom (see Table 1)

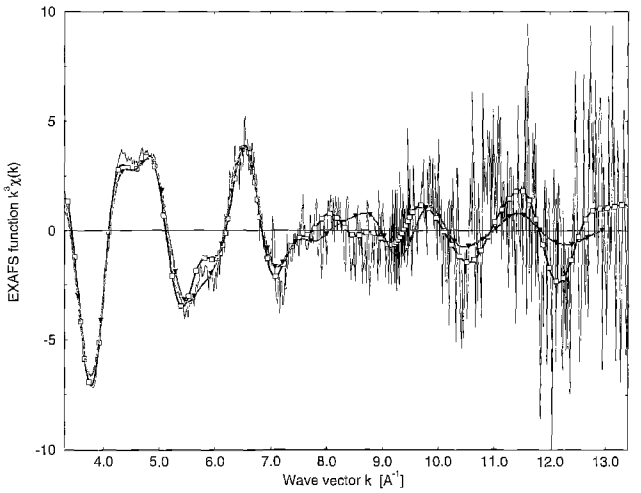

Fig. 8. EXAFS spectra of the *P. shermanii* Fe-SOD at pH 6.4 (*thin solid line*); *triangles:* theoretical curve calculated from the preliminary structure of the *E. coli* Fe-SOD refined with the EXAFS data of the *E. coli* Fe-SOD; *squares:* "constrained refinement" fit of the preliminary structure. Distances of the atoms in the first coordination shell as defined in Table 2: $R(O_1) = 1.86$ Å, $R(N_4) = 2.11$ Å, $R(N_9) = 2.09$ Å, $R(N_{14}) = 2.11$ Å, $R(O_{19}) = 1.96$ Å

Table 3. Iron – ligand distances in the first coordination shell at the different pH-values

Ligand	Atom	*P. shermannii*				*E. coli*
		pH 6.4	pH 7.8	pH 9.3	pH 10.0	pH 8.0
Aspartate	O_1	1.86 Å	1.87 Å	1.86 Å	1.86 Å	1.91 Å
Histidine I	N_4	2.11 Å	2.13 Å	2.14 Å	2.13 Å	2.16 Å
Histidine II	N_9	2.09 Å	2.14 Å	2.14 Å	2.15 Å	2.05 Å
Histidine III	N_{14}	2.11 Å	2.12 Å	2.13 Å	2.16 Å	2.07 Å
Water molecule	O_{19}	1.96 Å	1.98 Å	1.99 Å	1.98 Å	1.96 Å
Hydroxyl ion	O_{20}	–	2.09 Å	2.06 Å	2.07 Å	–

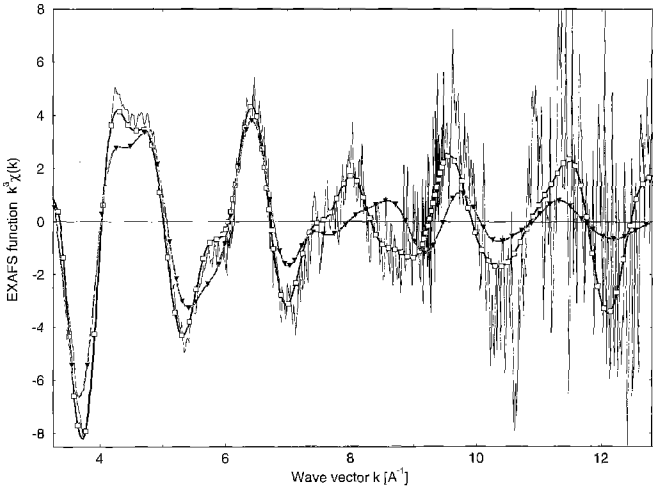

Fig. 9. EXAFS spectra of *P. shermanii* Fe-SOD at pH 7.8 (*thin solid line*); *triangles:* the theoretical curve is calculated from the preliminary structure of the *E. coli* Fe-SOD that was refined with the EXAFS data of the *E. coli* Fe-SOD; *squares:* "restrained refinement" structure after the introduction of an additional water as sixth ligand (represented by $R(O_{20})$). Distances of the atoms in the first coordination shell as defined in Table 2: $R(O_1) = 1.87$ Å, $R(N_4) = 2.13$ Å, $R(N_9) = 2.14$ Å, $R(N_{14}) = 2.12$ Å, $R(O_{19}) = 1.98$ Å, $R(O_{20}) = 2.09$ Å

active center. Only the distances of the ligands with respect to the iron are reduced in comparison to the *E. coli* Fe-SOD (see Table 3), the changes in the angles defining the exact atom positions are always less than two degrees.

Starting with the *E. coli* structure neither the "constrained" nor the "restrained refinement" yields a satisfactory fit for the experimental data for pH 7.8. The intensity of the first EXAFS oscillations and of the principal Fourier maximum cannot be reproduced (compare Figs. 9 and 10). Simulations have shown that the discrepancy can not be solved by varying the Debye-Waller factors or the amplitude reduction factor, *AFAC*. Since the pre-edge peak indicates six-fold coordination we increased the number of the coordinating ligands. An additional water molecule (or a hydroxyl ion which is even more likely since the amount of hydroxyl ions is increased at high pH and it has the same charge as the superoxide ion) could move into a sixth coordination site. In order to check this possibility the number of water molecules was varied. The best fit is obtained using the "restrained refinement" method and an independent determination of the positions of two oxygens i. e. one water and one hydroxyl ion. The result is displayed in Figs. 9 and 10. The aspartate is not shifted on going from pH 6.4 to pH 7.8, just the average iron-histidine distance changes from 2.10 Å to 2.13 Å (see Table 3). The addition of one water molecule is the easiest way to get a good fit of the data without another change of the iron environment obtained at pH 6.4. This is no proof that other explanations are impossible. It has been shown for four-coordinated systems that the pre-edge peak area changes noticeably if the geometry of the site is drastically altered, e.g. planar to tetragonal (Shadle et al. 1993). However, we could not find evidence for a drastic distortion in our data; on the contrary, the geometry is practically conserved. One may speculate that the water molecule found at pH 6.4 is de-

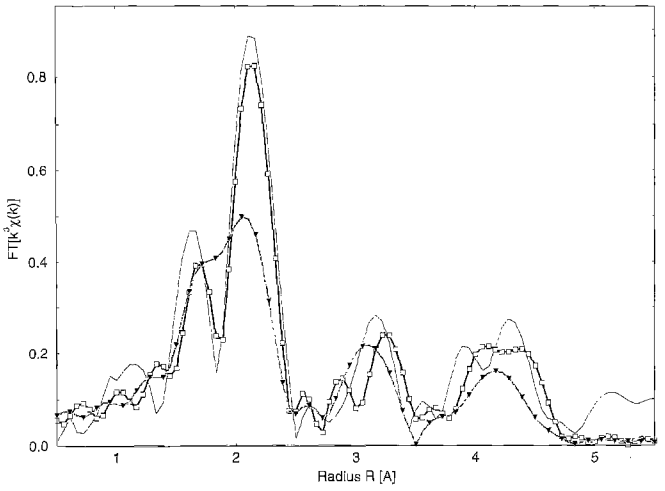

Fig. 10. Fourier transform of the EXAFS spectra of *P. shermanii* Fe-SOD at pH 7.8 (*thin solid line*); triangles: theoretical curve calculated from the refined structure of the *E. coli* Fe-SOD; *squares:* "restrained refinement" structure obtained after the introduction of an additional water molecule. Distances of the atoms in the first coordination shell as defined in Table 2: $R(O_1)=1.87$ Å, $R(N_4)=2.13$ Å, $R(N_9)=2.14$ Å, $R(N_{14})=2.12$ Å, $R(O_{19})=1.97$ Å, $R(O_{20})=2.09$ Å

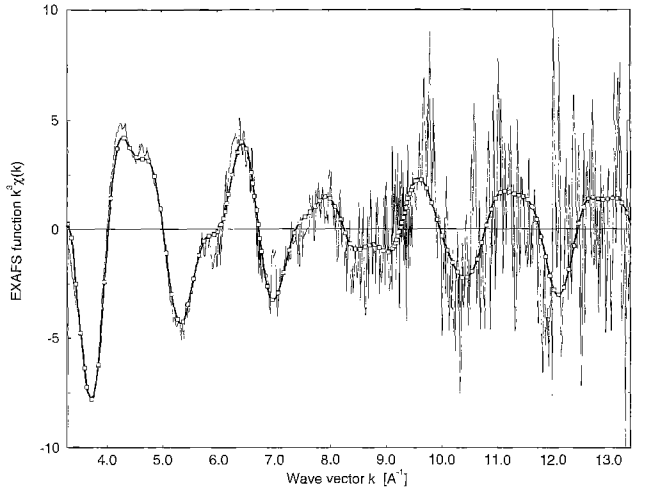

Fig. 11. EXAFS spectra of *P. shermanii* Fe-SOD at pH 9.3; the experimental spectrum (*thin solid line*) compared to the theoretical curve after a "restrained refinement" with a sixth ligand (*squares*). Distances of the atoms in the first coordination shell as defined in Table 2: $R(O_1)=1.86$ Å, $R(N_4)=2.14$ Å, $R(N_9)=2.14$ Å, $R(N_{14})=2.13$ Å, $R(O_{19})=1.99$ Å, $R(O_{20})=2.06$ Å

protonated at higher pH-values changing the coordination of the iron. The carboxylate group of the aspartate could turn so that the second oxygen of this group (OD 1) could form a quasi sixth ligand. But it is exactly the water molecule which keeps the carboxylate group in place by hydrogen bonds. The comparison of the Fourier transform shows that with respect to *E. coli* the spread in the distances of the histidines is reduced for the *P. shermanii* SOD at pH 7.8. This is reflected by the narrow and pronounced first Fourier maximum (see Fig. 10). The enlargement of the area of this maximum is also evident.

The similarity of the absorption spectra at pH 7.8 and 9.3 already suggests an identical approach to the interpre-

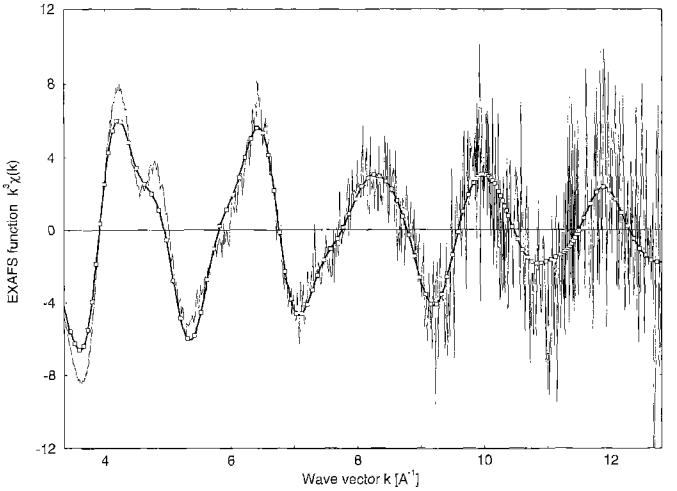

Fig. 12. Zn EXAFS spectrum of *P. shermanii* SOD at pH 6.4 (*thin solid line*); *squares:* theoretical curve fitted by "constrained refinement" from the refined structure of the *E. coli* Fe-SOD. Distances of the atoms in the first coordination shell as defined in Table 2: $R(O_1)=1.91$ Å, $R(N_4)=2.03$ Å, $R(N_9)=2.04$ Å, $R(N_{14})=2.02$ Å, $R(O_{19})=1.96$ Å

tation of the EXAFS spectrum at the highest pH-value investigated. Again a six-fold coordination is evident, the results are shown in Fig. 11. As expected, the shifts of the iron-ligand distances between 7.8 and 9.3 after a "restrained refinement" remain negligible (see Table 3).

Figure 12 shows the EXAFS spectrum of the zinc superoxide dismutase from *P. shermanii* measured at pH 6.4. As in the case of the Fe-SOD at pH 6.4 the "constrained refinement" of the *E. coli* starting structure yields a good fit and coincides in coordination number with the results obtained for the ferric SOD at this pH. This clearly demonstrates that the zinc is indeed replacing the iron atom in the active center. In this case the zinc-ligand distances are different from the Fe-SOD, the aspartate is situated at 1.91 Å from the zinc (iron: 1.86 Å), the imidazole rings at about 2.03 Å (iron: 2.10 Å). The differences of the distances of the aspartate and imidazole rings in the first coordination shell are clearly reduced which is easily visible also in an unsplit first Fourier maximum.

Discussion

The interpretation of the X-ray absorption data of the ferric SOD of *P. shermanii* reveals a structure that is very similar to the structure of the *E. coli* Fe-SOD. Particularly, at pH 6.4 the structure of the *P. shermanii* SOD and the *E. coli* SOD at pH 8.0 show practically no differences in the number and geometrical orientation of the ligands. Therefore, the ligands of the iron atom in the active center of the *P. shermanii* Fe-SOD are three histidines, one aspartate and one water molecule. Apart from geometrical orientation, there is evidence for distance differences between the two types of ferric SOD. The simulation of the EXAFS spectra and the shape of the first maximum of the Fourier transformed spectra at all pH-values imply that the differences in the distances between the histidines and

the iron atom is reduced compared to the *E. coli* Fe-SOD. For the *E. coli* Fe-SOD the histidines vary from 2.05 Å to 2.16 Å in distance whereas all the histidines of the *P. shermanii* Fe-SOD are situated roughly at the same distance. At pH 6.4 the histidines are all at about 2.10 Å from the iron, at pH 9.3 at about 2.14 Å. They all seem to behave equally at each observed pH-value (see Table 3).

The pH dependence of the structure of *P. shermanii* SOD reveals itself both in the 1s→3d pre-edge transition which is connected to the geometry of the active center (Roe et al. 1984) and in the EXAFS region of the spectra. With increasing pH the coordination number rises from five to six. Apparently, we observed a transition between two configurations of the atoms near the active center. At low pH-values a five ligated state dominates. At high pH-values a six ligated, almost inactive form is found. These two states are in a pH dependent equilibrium. Along with the transition the oxygen atom of the carboxyl group of the aspartate as well as the fifth ligand, the water molecule, do not change their bond length. The average over the bond lengths of the three imidazole groups increases by about 0.04 Å from pH 6.4 to 9.3 and this process continues even on going to pH 10.0 (see Table 3). However, the resolution of the EXAFS spectra is not sufficient to separate the contributions of each particular imidazole ring. The imidazole groups remain interchangeable without affecting the accuracy of the theoretical calculation of the EXAFS spectra. For the *E. coli* Fe-SOD this increase in coordination number has been proposed recently (Tierney et al. 1995), but the transition seems to take place at higher pH-values in that case. At the observed pH 8.0 the *E. coli* Fe-SOD is still in the five coordinated state whereas the *P. shermanii* Fe-SOD is already found in the six coordinated state at pH 7.8. This behavior is consistent with the pH dependence of the activity of the *P. shermanii* Fe-SOD. The activity decreases by about a factor of five between the pH-values 6.4 and 7.8 and by about a factor of 2 between pH 7.8 and pH 9.3 (Meier et al. 1995). Again the major changes occur between pH 6.4 and pH 7.8. The reduced activity can be explained by the presence of the additional ligand which blocks the pathway to the iron atom and makes it more difficult or impossible for the superoxide ion to reach the binding site.

Acknowledgements. This work was supported by the Deutsche Forschungsgemeinschaft, by DESY, Projektträger Synchrotronstrahlung des BMFT, the EMBL and the Fonds der Chemie.

References

Achterhold K (1995) Ph. D. Thesis, Technical University Munich, Germany

Binsted N, Campbell JW, Gurman SJ, Stephenson PC (1991) SERC Daresbury Laboratory EXCURV92 Program, using: Gurman SJ, Binsted N, Ross I (1984) J Phys C 17: 143–151; Gurman SJ, Binsted N, Ross I (1986) J Phys C 19: 1845–1861; Gurman SJ (1988) J Phys C 21: 3699–3717; Joyner RW, Martin KJ, Meehan P (1987) J Phys C 20: 4005–4012; Binsted N, Strange RW, Hasnian SS (1992) Biochemistry 31: 12117–12125

Binsted N, Strange RW, Hasnain SS (1992) Constrained and restrained refinement in EXAFS data analysis with curved wave theory. Biochemistry 31: 12117–12125

Di Pace A, Cupane A, Leone M, Vitorano E, Cordone L (1992) Vibrational coupling, spectral broading mechanisms and anharmonicity effects in carbonmonoxy heme proteins studied by the temperature dependence of the Soret band line shape. Biophys J 63: 475–484

Jones A (1994) O-Program, Version 5.10.2, Uppsala University, Sweden

Lah MS, Dixon MM, Pattridge KA, Stallings WC, Fee JA, Ludwig ML (1995) Structure – Function in Escherichia coli Iron Superoxide Dismutase: Comparisons with Manganese Enzyme from Thermus thermophilus. Biochemistry 34: 1646–1660

Lee PA, Beni G (1977) New method for the calculation of atomic phase shifts: Application to extended X-ray absorption fine structure (EXAFS) in molecules and crystals. Phys Rev B 15: 2862–2883

Ludwig ML, Metzger AL, Pattridge KA, Stallings WC (1991) Manganese superoxide dismutase from Thermus thermophilus: A structural model refined at 1.8 Å resolution. J Mol Biol 219: 335–358

Meier B, Barra D, Bossa F, Calabrese L, Rotilio G (1982) Synthesis of either Fe- or Mn-superoxide dismutase with an apparently identical protein moiety by an anaerobic bacterium dependent on the metal supplied. J Biol Chem 257: 13977–13980

Meier B, Michel C, Saran M, Huettermann J, Parak F, Rotilio G (1995) Kinetic and spectroscopic studies on a superoxide dismutase from Propionibacterium shermanii which is active with iron or manganese: pH dependence. Biochem J 310: 945–950

Parak F, Frauenfelder H (1993) Protein dynamics. Physica A 201: 332–345

Pettifer RF, Hermes C (1985) Absolute Energy Calibration of X-ray Radiation from Synchrotron Sources. J Appl Crystallogr 18: 404–412

Ringe D, Petsko GA, Yamakura F, Suzuki K, Ohmori D (1983) Structure of iron superoxide dismutase from Pseudomonas ovalis at 2.9 Å resolution. Proc Natl Acad Sci USA 80: 3879–3883

Roe AL, Schneider DJ, Mayer RJ, Pyrz JW, Widom J, Que Jr L (1984) X-ray absorption spectroscopy of iron-tyrosinate proteins. J Am Chem Soc 106: 1676–1681

Shadle SE, Penner-Hahn JE, Schugar HJ, Hedman B, Hodgson KO, Solomon EI (1993) X-ray Absorption Spectroscopic Studies of Blue Copper Site: Metal and Ligand K-Edge Studies to Probe the Origin of the EPR Hyperfine Splitting in Plastocyanin. J Am Chem Soc 115: 767–776

Shulman RG, Yafet Y, Eisenberger P, Blumberg WE (1976) Observation and interpretation of X-ray absorption edges in iron compounds and proteins. Proc Natl Acad Sci USA 73: 1384–1388

Stallings WC, Powers TB, Pattridge KA, Fee JA, Ludwig ML (1983) Iron superoxide dismutase from Escherichia coli at 3.1 Å resolution: A structure unlike that of copper/zinc protein at both monomer and dimer levels. Proc Natl Acad Sci USA 80: 3884–3888

Stallings WC, Pattridge KA, Strong RK, Ludwig ML (1984) Manganese and Iron Superoxide Dismutase are structural homologues. J Biol Chem 259: 10695–10699

Stallings WC, Pattridge KA, Strong RK, Ludwig ML (1985) The structure of manganese superoxide dismutase from Thermus thermophilus HB 8 at 2.4 Å resolution. J Biol Chem 260: 16424–16432

Stoddard BL, Howell PL, Ringe D, Petsko GA (1990) The 2.1 Å resolution structure of iron superoxide dismutase from Pseudomonas ovalis. Biochemistry 29: 8885–8893

Strange RW, Blackburn NJ, Knowles PF, Hasnian SS (1987) X-ray absorption spectroscopy of metal-histidine coordination in metalloproteins. Exact simulation of the EXAFS of Tetrakis(imidazole)copper(II) Nitrate and other Copper-imidazole complexes by use of a multiple-scattering treatment. J Am Chem Soc 109: 7157–7162

Tainer JA, Getzoff ED, Beem KM, Richardson JS, Richardson DC (1982) Determination and Analysis of a 2 Å Structure of Copper, Zinc Superoxide Dismutase. J Mol Biol 160: 181–217

Teo BK (1986) EXAFS: Basic Principles and Data Analysis. Springer, Berlin Heidelberg New York

Tierney DL, Free JA, Ludwig ML, Penner-Hahn JE (1995) X-ray Absorption Spectroscopy of the Iron Site in Escherichia coli Fe(III) Superoxide Dismutase. Biochemistry 34: 1661–1668